JOURNAL OF BACTERIOLOGY, Aug. 1996, p. 4461–4471 Vol. 178, No. 15
0021-9193/96/$04.00+0

An Alternative Pathway of Recombination of Chromosomal Fragments Precedes *recA*-Dependent Recombination in the Radioresistant Bacterium *Deinococcus radiodurans*

MICHAEL J. DALY AND KENNETH W. MINTON*

F. E. Hébert Medical School, Uniformed Services University of the Health Sciences, Bethesda, Maryland 20814-4799

Received 11 March 1996/Accepted 21 May 1996

Deinococcus radiodurans **R1 and other members of this genus are able to repair and survive extreme DNA damage induced by ionizing radiation and many other DNA-damaging agents. The ability of R1 to repair completely >100 double-strand breaks in its chromosome without lethality or mutagenesis is *recA* dependent. However, during the first 1.5 h after irradiation, *recA*$^+$ and *recA* cells show similar increases in the average size of chromosomal fragments. In *recA*$^+$ cells, DNA continues to enlarge to wild-type size within 29 h. However, in *recA* cells, no DNA repair is observed following the first 1.5 h postirradiation. This *recA*-independent effect was studied further, using two slightly different *Escherichia coli* plasmids forming adjacent duplication insertions in the chromosome, providing repetitive sequences suitable for circularization by non-*recA*-dependent pathways following irradiation. After exposure to 1.75 Mrad (17,500 Gy), circular derivatives of the integration units were detected in both *recA*$^+$ and *recA* cells. These DNA circles were formed in the first 1.5 h postirradiation, several hours before the onset of detectable *recA*-dependent homologous recombination. By comparison, *D. radiodurans* strains containing the same *E. coli* plasmids as nonrepetitive direct insertions did not form circular derivatives of the integration units before or after irradiation in *recA*$^+$ or *recA* cells. The circular derivatives of the tandemly integrated plasmids were formed before the onset of *recA*-dependent repair and have structures consistent with the hypothesis that DNA repair occurring immediately postirradiation is by a *recA*-independent single-strand annealing reaction and may be a preparatory step for further DNA repair in wild-type *D. radiodurans*.**

Deinococcus (formerly *Micrococcus*) *radiodurans* is the most ionizing-radiation resistant organism discovered to date (21). The resistance of *D. radiodurans* has been shown to be due to exceedingly efficient DNA repair (19, 21). For example, following a radiation exposure to 1.0 Mrad (10,000 Gy), pulsed-field gel electrophoresis (PFGE) shows that *D. radiodurans* sustains about 100 double-strand breaks (DSBs) per chromosome, which it repairs without lethality, mutagenesis, or rearrangements within 29 h. Most other organisms cannot survive two or three DNA radiation-induced DSBs per chromosome (7, 8, 25).

Complete DSB rejoining in *D. radiodurans* is *recA* dependent, as demonstrated by the requirement for *recA* to restore chromosomal integrity from many hundreds of DNA fragments (5, 7). However, in the current study, we show that *recA*-deficient *D. radiodurans* is able to rejoin many DSBs in a sequence-specific manner within the first 1.5 h following irradiation, presumably by a *recA*-independent recombination pathway. The identical kinetics of fragment rejoining in *recA*$^+$ and *recA* cells at early times following irradiation suggests that this *recA*-independent pathway precedes *recA*-dependent homologous recombination.

Irrespective of whether repair of DSBs proceeds by *recA*-dependent or *recA*-independent means, or both, DSB homologous repair requires redundant information, which is readily available in *D. radiodurans*. *D. radiodurans* contains 4 identical chromosomal copies during stationary phase and 10 identical chromosomal copies during exponential phase (15). Although the redundancy of chromosomal copy number is not itself sufficient to provide the extreme radioresistance of *D. radiodurans* (19), the presence of redundant information provides the necessary homology for the action of any recombinational DNA repair pathways employed by this organism.

* Corresponding author. Mailing address: F. E. Hébert Medical School, Uniformed Services University of the Health Sciences, 4301 Jones Bridge Road, Bethesda, MD 20814-4799. Phone: (301) 295-3476. Fax: (301) 295-1640. Electronic mail address: minton@usuhsb.usuhs.mil.

MATERIALS AND METHODS

Bacterial strains, growth, and transformation. *D. radiodurans* R1 is wild type (1), and the *D. radiodurans* R1 derivative, rec30, was obtained by chemical mutagenesis using *N*-methyl-*N*′-nitro-*N*-nitrosoguanidine (22) and shown to be defective in the *D. radiodurans recA* gene (11). *Deinococcus*-derived DNA fragments used to construct the integrative plasmids for *D. radiodurans* R1 are from (i) the *D. radiodurans* SARK plasmid derivatives pI3 and pS19, both of which have little homology with R1 chromosomal sequences and do not recombine with the R1 chromosome (17, 28); and (ii) a R1 sequence derived from chromosomal locus 11 (pS11 [29]) which allows plasmid integration into the chromosome. *D. radiodurans* was grown in TGY broth (0.8% Bacto Tryptone, 0.1% glucose, 0.4% Bacto Yeast Extract [Difco Laboratories]) at 32°C with aeration or on TGY plates solidified with 1.5% agar. *Escherichia coli* DH10B (Life Technologies) was grown in Luria-Bertani (LB) broth or on LB plates solidified with 1.5% agar. The selective drug concentration for *D. radiodurans* was 3 μg of chloramphenicol per ml, 8 μg of kanamycin per ml, or 2.5 μg of tetracycline per ml. Selective drug concentrations for *E. coli* were 50 μg of ampicillin per ml or 30 μg of tetracycline per ml. *E. coli* was transformed by the $CaCl_2$ technique. Transformation of *D. radiodurans* was also by a $CaCl_2$-dependent technique described previously (18).

DNA isolation and manipulation. Purification of plasmid and chromosomal DNA from *D. radiodurans* and *E. coli*, enzymatic reagents, pulsed-field gel electrophoresis (PFGE), conventional gel electrophoresis, blotting, hybridization, washing of blots, and autoradiography were as described previously (7, 16, 29). The probe used in Southern blot experiments is the pBR322 *tet* gene, extending from the *Eco*RI site just upstream of *tet* to an 8-bp *Xho*I-5 linker inserted at nucleotide position 1268 of pBR322 at the end of the *tet* gene (7–9). Radiolabeling of the probe was by the random priming technique.

Construction of strains MD409, MD417, MD424, and MD431. MD424 and MD431 (Fig. 1), the strains used in this study, are transformation products of strains MD409 and MD417. Consequently, the construction of these latter two is described before that of MD424 and MD431. The relevant chromosomal region of all four strains is shown in Fig. 1A. To construct MD417, the *Pvu*II site of the

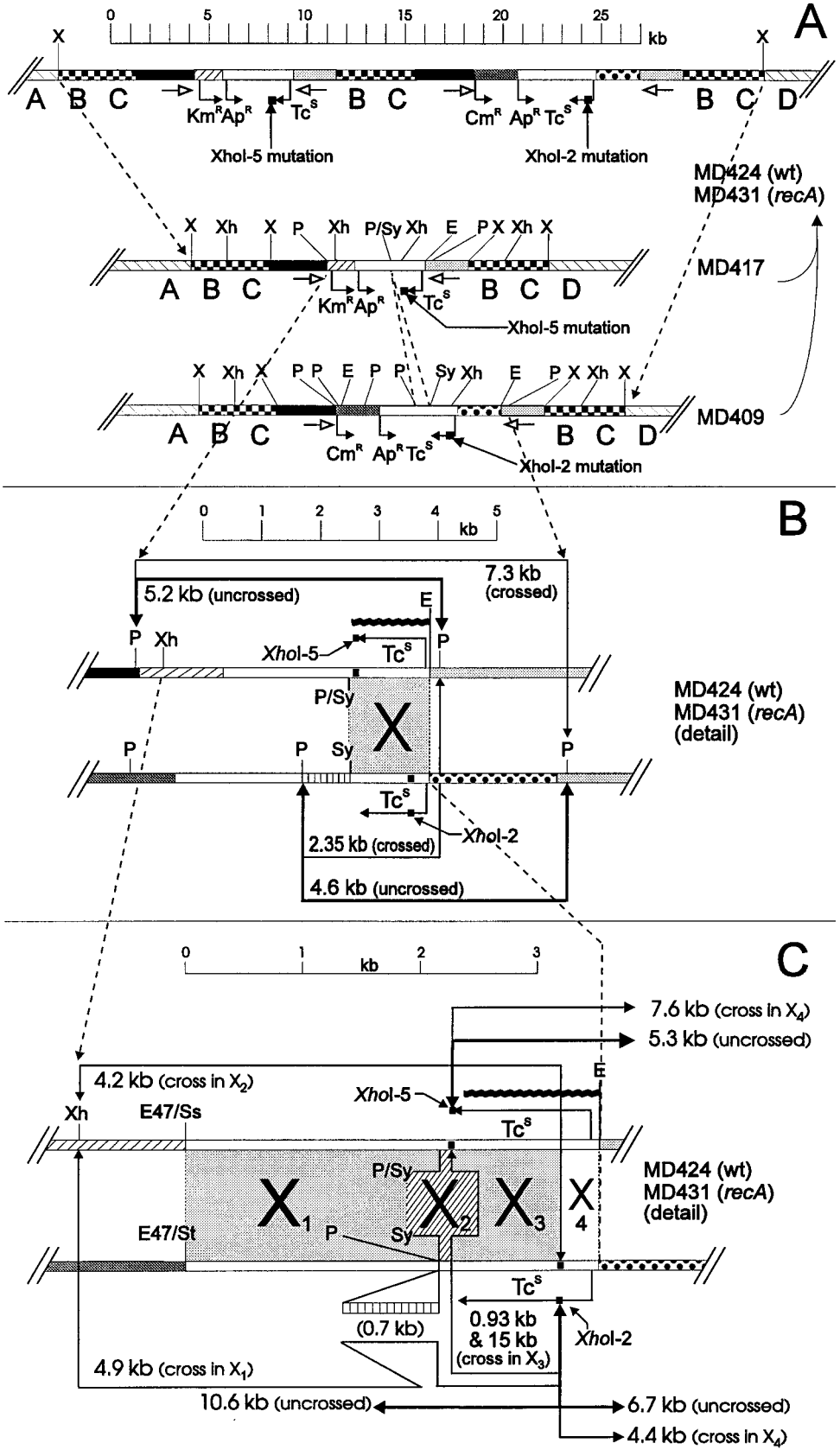

3.9-kbp *Pvu*II-*Xba*I fragment of pS11 (BC) (Fig. 1A) was converted to an *Xba*I site by the addition of an *Xba*I linker. This 3.9-kbp *Xba*I fragment was inserted into the *Xba*I site of pMD297 (8) to give pMD417 (13.8 kbp). Transformation of this plasmid into wild-type R1 and selection for Km^r gave strain MD417 (Fig. 1A). Strain MD409 is similar to strain MD417 (Fig. 1A) except for the use of a Cm^r-Tc^s cassette in MD409 instead of the Km^r-Tc^s cassette that is present in MD417.

The construction of MD409 was complicated because of lack of useful restriction sites and is summarized as follows. The starting materials were pMD186, pMD294, and pMD300, all described previously (8). The *Xba*I site of pMD294 (8) was destroyed by Klenow enzyme fill-in and subsequent ligation to give pMD329 (8.4 kbp). pMD211 is the self-ligated *Sac*II fragment (11 kbp) of pMD186 (8). The unique *Sac*II site of pMD211 was converted to an *Xba*I site by T4 DNA polymerase fill-in of the site, followed by the addition of *Xba*I linkers to give pMD249. pMD331 was formed by ligation of *Eco*RI-cleaved pMD329 (see above) to the *Eco*RI fragment (5.0 kbp) of pMD249. The 3.9-kbp *Xba*I fragment of pMD417 (see above) that contains the chromosomal sequence (BC) was inserted into the *Xba*I site of pMD331 to give pMD409, in which the orientation of the 3.9-kbp *Xba*I fragment was the same as in pMD417. Strain MD409 was constructed by transformation of pMD409 (17.7 kbp) into wild-type *D. radiodurans* cells with selection for Cm^r. The structure of MD409 is shown in Fig. 1A.

Strains MD424 (*recA*$^+$) and MD431 (*recA*) were constructed such that both contained the Km^r-Tc^s and Cm^r-Tc^s cassettes (8). The cassettes were inserted next to each other in the chromosome by tandem duplication. Strain MD424 was obtained by transformation of MD417 with genomic DNA prepared from MD409. Double selection was for both Km^r and Cm^r. The *recA* equivalent of MD424, strain MD431, was obtained by transforming strain rec30 (*recA*) with MD424 genomic DNA and subjecting it to double selection for both Cm^r and Km^r. The tandem duplication structures and orientation were determined by Southern blot analysis using appropriate restriction enzyme cleavages and probes (not shown).

Construction of strains MD399 and MD425. MD399 is a previously constructed *recA*$^+$ strain (5) containing a direct insertion of the Cm^r-Tc^s cassette at locus 11 (Fig. 2). MD425 is identical to MD399 except that it is *recA* (Fig. 2). MD425 was obtained by transformation of strain rec30 with high-molecular-weight DNA prepared from MD399 followed by selection for Cm^r. The structure of MD425 was confirmed by Southern blot analysis using appropriate restriction enzymes cleavages and probes (not shown).

Measurements of time course of repair and recombination. Early-stationary-phase cells from overnight cultures (approximately 10^8 cells per ml) were irradiated on ice without change of broth to 1.75 Mrad at a rate of 1.0 Mrad/h, using a ^{60}Co source, then diluted 1/50 in fresh TGY medium without selective drugs, and incubated at 32°C with aeration. Samples were taken at the times indicated. Visible cell counts were determined with a hemocytometer as described previously (7). Viable cell counts and Tc^r recombinant cell counts were determined by plating for colonies on nonselective TGY agar plates and tetracycline-supplemented TGY agar plates. Plates were incubated for at least 3 days before counting colonies. *E. coli* transforming activity of the artificial chromosomal repeats during the course of repair was determined by transformation of purified *D. radiodurans* genomic DNA into *E. coli* DH10B as described previously (7).

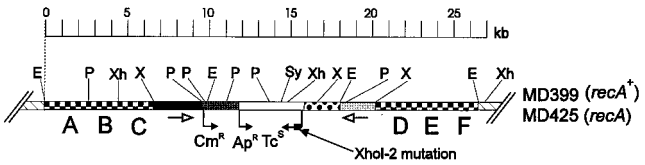

FIG. 2. Regional chromosomal map of MD399 and MD425 illustrating plasmid direct integration at locus 11 and function. MD399 is a previously constructed *recA*$^+$ strain (5) containing a direct insertion of the Cm^r-Tc^s cassette at chromosomal locus 11. MD425 (*recA*) was obtained by transforming MD399 chromosomal DNA into rec30 followed by selection for Cm^r. Abbreviations and shading are as described in the legend to Fig. 1.

RESULTS

Characteristics of MD417 and MD409. The integrative vectors pMD417 and pMD409 were inserted in the same cells at the same randomly selected chromosomal site (locus 11) to yield strains MD424 (in *recA*$^+$ R1 recipients) and MD431 (in *recA* strain rec30 recipients) (Fig. 1A) as described in Materials and Methods. The site of integration, locus 11, acquires its name from pS11, an integrative vector that contains the chromosomal sequence arbitrarily designated (BC) or locus 11 (Fig. 1A). pS11 has been used previously as an integrative vector for making insertions by tandem duplication (12, 13). In this configuration, the integrated plasmids, referred to as segments 417 and 409, were designed to assess both fragment circularization and chromosomal recombination, induced by γ irradiation. These segments contain the identical flanking strain R1 chromosomal sequences (BC) (Fig. 1A). However,

FIG. 1. Regional chromosomal maps of MD424 and MD431 illustrating plasmid tandem integration at locus 11, functions, and restriction fragments indicative of recombination. (A) Map of integrated plasmids pMD417 and pMD409. In *D. radiodurans*, chromosomal segment 417 can confer Km^r (*aphA*) because of the deinococcal promoting sequences in the fragment derived from the *D. radiodurans* SARK natural plasmid pUE11 (solid region) that is joined to a portion of the *E. coli* plasmid pMK20 (diagonally hatched fragment) that contains the *aphA* gene (Km^r). In *D. radiodurans*, segments 417 and 409 can confer Tc^r (if the *tet* gene recombines to wild type [wt]) because of the promoting sequences in a region derived from another SARK natural plasmid, pUE10 (light gray area). The *tet* gene is located within the sequence derived from pBR322 (white region). In *D. radiodurans*, segment 409 expresses *cat* (Cm^r) as a result of the *cat* gene in a fragment from pKK232-8 (3) (dark gray region) and the adjacent pUE11 promoting sequences. Circular derivatives of segments 417 and 409 cannot replicate as plasmids in *D. radiodurans* because of the absence of a deinococcal plasmid origin of replication. In *E. coli*, circular derivatives of segments 417 and 409 can replicate as a result of the pBR322 replication origin. In *E. coli*, the *tet* genes can express Tc^r (if recombined to wild type) as a result of *E. coli* promoting sequences present immediately upstream of *tet*. Also, in *E. coli*, pMD417 confers Km^r because of the *E. coli* pMK20-derived promoting sequences immediately upstream of *aphA*. For any gene, such as *aphA*, to be expressed in both *E. coli* and *D. radiodurans*, two sets of promoting sequences are necessary, one for *D. radiodurans* and one for *E. coli*, because *D. radiodurans* and *E. coli* recognize each other's promoters very poorly (30). In *E. coli*, pMD409 and pMD417 confer Ap^r because of the *bla* gene in pBR322. pMD409 does not express Cm^r in *E. coli* in low abundance because of the lack of an *E. coli* promoting sequence for this gene (3). The dotted region (not checkered), which indicates the introduction of a physical polymorphism that can be seen by restriction digestions, is a rat cDNA fragment from pGABI that encodes a rat biliary glycoprotein, lacking homology to *D. radiodurans* or pBR322 DNA. The checkered segments are the duplicated chromosomal regions (BC). Open-headed arrows indicate deinococcal promoting sequences. Filled arrows indicate drug resistance determinants as labeled. The 695-bp *Pvu*II-*Sty*I region that is deleted from the pBR322 portion of segment 417 is indicated by dotted lines between segments 417 and 409, connecting the *Pvu*II-*Sty*I region of 409 to the *Pvu*II-*Sty*I fusion site in 417. This deletion does not affect function, but like the fragment of rat cDNA, the deletion was introduced to yield a physical polymorphism that can be followed by appropriate restriction digestions. Restriction site abbreviations: E, *Eco*RI; P, *Pvu*II; P/Sy, *Pvu*II-*Sty*I fusion; Sy, *Sty*I; X, *Xba*I; Xh, *Xho*I. (B) Detail of pBR322 regions and flanking regions of segments 417 and 409 in MD424 and MD431, showing expected *Pvu*II restriction fragments, made visible by use of the *tet* gene probe. The *Pvu*II restriction digestion yields fragments indicative of crossover or lack of crossover within the region of homology (gray field) labeled X, because of the flanking polymorphisms; gene conversions are not detected by the *Pvu*II digestion. The probe, indicated by a wavy black line, is the 1.2-kbp *Eco*RI-*Xho*I fragment from pRDK39 that consists of the *tet* gene (7–9). Parental fragments visible by autoradiography are 5.2 kbp (from 417) and 4.6 kbp (from 409). Fragments indicative of crossover are 7.3 and 2.35 kbp. These two latter fragments can be generated by a crossover or annealing but not by a gene conversion. The locations of the *Xho*I-2 mutation in segment 409 (pBR322 site 339 in the *tet* gene) and the *Xho*I-5 mutation in 417 (pBR322 site 1268 in the *tet* gene; a 929-base window) are indicated. Both mutations consist of an 8-bp *Xho*I linker inserted into *Taq*I sites (8, 9). The segments' shading is as described for panel A, with the addition that the vertically hatched region indicates the *Pvu*II-*Sty*I 695-bp sequence of pBR322 that is present in segment 409 but deleted in 417. Restriction site abbreviations are the same as in panel A. (C) Detail of panel B showing pBR322 regions and flanking regions of segments 417 and 409, showing expected *Xho*I restriction fragments, made visible by use of the same *tet* gene probe. The *Xho*I restriction digestion generates various different-length fragments predicted by recombination, depending on whether the crossover occurred in X_1, X_2, X_3, or X_4. Parental fragments are 10.6 and 6.7 kbp from segment 409 and 5.3 kbp from segment 417. Fragments indicative of recombination include 4.9 kbp if there is a crossover in the 2-kbp region X_1, 4.2 kbp if a crossover occurs in the 101-bp region X_2, 0.93 and 15 kbp if a crossover occurs within the 929-bp region X_3, and 7.6 and 4.4 kbp if a crossover occurs within the 339-bp region X_4. Fragments, restriction sites, probe, and sites of mutation in the *tet* gene are as described for panel A. Unlike the case for the *Pvu*II digestion, the results of the *Xho*I digestion can be obtained by gene conversion of the *Xho*I-2 and/or *Xho*I-5 sites of *tet* mutation to wild type, and detection is not solely limited to crossover or annealing events.

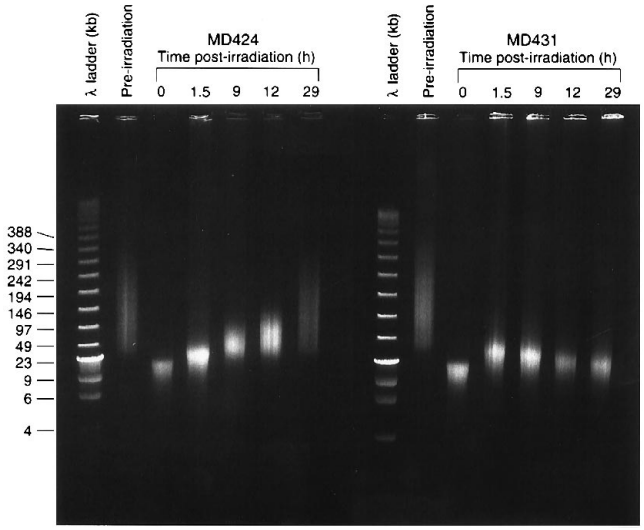

FIG. 3. PFGE of chromosomal DNA prepared from MD424 (*recA*$^+$) and MD431 (*recA*). Cultures of MD424 and MD431 were grown to early stationary phase and γ irradiated on ice without change of broth with ^{60}Co to 1.75 Mrad. Total genomic DNA was prepared by the miniprep technique immediately afterward, or the cells were diluted 1/50 in fresh non-drug-selective TGY medium and incubated at 32°C with aeration for 1.5 to 29 h, and genomic DNA was prepared by the same technique. PFGE conditions are as described previously (7). Each lane contains the DNA from about 3×10^6 cells, as determined by counting with a hemocytometer (7). The DNA is visualized by ethidium bromide staining. The markers are composed of a λ ladder plus λ phage DNA digested with *Hin*dIII. The increase in size of DNA fragments at the 1.5-h time point is approximately from 20 kbp (0 h postirradiation) to 30 kbp (1.5 h postirradiation). Severe fragmentation of DNA is apparent in both MD424 and MD431, and both are partially repaired at the 1.5-h time point. At later times, only MD424 undergoes further repair.

segments 417 and 409 differ within their *E. coli*-derived sequences in three ways.

(i) Different drug resistance determinants. Segment 417 contains and expresses the *aphA* gene (Km^r) but not the *cat* gene (Cm^s), while for segment 409, the reverse is true. This facilitates the selection for retention of both segments in *D. radiodurans* by use of double drug selection with both chloramphenicol and kanamycin.

(ii) Physical polymorphisms. Segments 417 and 409 are physically polymorphic in the region of the *tet* gene, containing flanking sequences that differ both upstream of *tet* (a 2.2-kbp insertion of rat cDNA in segment 409) and downstream of *tet* (a 695-bp *Sty*I-*Pvu*II deletion of pBR322 DNA in segment 417) (Fig. 1A). These polymorphisms allow for detection of recombination in this region by restriction cleavage and Southern blot analysis.

(iii) Allelic polymorphisms in the *tet* gene. Segment 417 is Tc^s as a result of the presence of the *Xho*I-5 mutation in the *tet* gene, consisting of an 8-bp *Xho*I linker inserted at nucleotide position 1268 of pBR322. Segment 409 is Tc^s as a result of the *Xho*I-2 mutation, consisting of the same linker inserted at pBR322 nucleotide position 339 in the *tet* gene. These mutations are 929 bp apart, allowing for detection of recombination in *D. radiodurans* (both crossover or gene conversion) by selecting for Tc^r (8, 9).

We determined the levels of postirradiation survival of MD424 and MD431 and found that they were identical to those of *recA*$^+$ wild-type R1 and *recA* rec30 cells, respectively (not shown). Thus, the radioresistance of these strains was unaffected by the tandem duplications.

The early phase of postirradiation DSB mending. An exposure to 1.75 Mrad is used here because it is the D_{37} of wild-type *D. radiodurans* in our standard conditions. The D_{37} is the dose required to achieve 37% survival of CFU, statistically equivalent to one lethal hit per cell, and therefore is closely related to the maximum cellular repair capacity. In addition, this exposure produces little effect on postirradiation growth of cells because the original number of cells (100%) is restored by only 1.4 generations of growth (about 1.4 h) (7, 8).

In preparation of high-molecular-weight DNA for PFGE, rather than embedding the organisms in agar, we gently purified DNA in liquid (7, 19). The reason for liquid DNA purification is to avert the retention of DNA in the agarose plugs during PFGE, which can occur unpredictably in DNA from any organism in any lane (e.g., reference 24). While retention is not problematic in chromosomal mapping, it can be a severe liability for strand break rejoining studies. The chromosome size is about 3×10^6 bp (15), and the average size of DNA fragments in the unirradiated sample is about 1.4×10^5 bp (Fig. 3), indicating that purification in liquid introduced about 21 DSBs per chromosome. The 0-h postirradiation sample shows DNA fragments that are about 2.0×10^4 bp or less, as reported previously (7, 19), indicating at least 150 DSBs per chromosome. Since the maximum-sized fragments after irradiation are smaller than the minimum-sized fragments generated by shearing of DNA from unirradiated cells, it is likely that few or no DSBs (caused by shearing) are generated in the 0-h postirra-

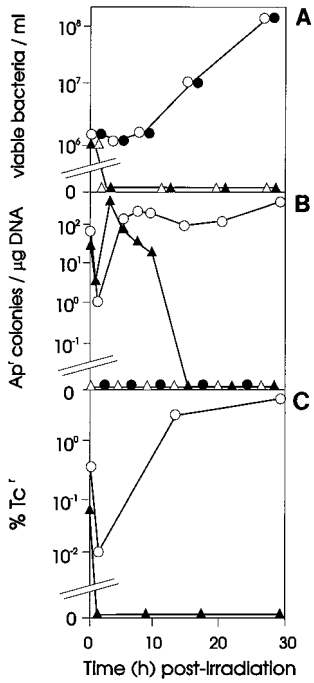

FIG. 4. Viable cells, transforming activity, and percentage Tc^r recombinants for strains MD424, MD431, MD399, and MD425. Early-stationary-phase cells (~10^8/ml) were exposed to 1.75 Mrad on ice, then diluted 1/50 in fresh TGY medium, and allowed to incubate at 32°C for the indicated times. Viable cell counts (A) were determined by plating for colony formation at the times indicated. Genomic DNA transforming activity (B) was determined by purification of total DNA by the miniprep technique. At the times indicated, 1 μg of DNA was used to transform *E. coli* DH10B to Ap^r as determined by plating on selective agar. *D. radiodurans* Tc^r recombinant cell counts (C) were determined by plating for colony formation on TGY medium supplemented with tetracycline at the times indicated and are expressed as a percentage of the viable count. Note that an exposure to 1.75 Mrad is lethal to *recA D. radiodurans* strains. Open circles, MD424 (*recA*$^+$); solid triangles, MD431 (*recA*); solid circles, MD399 (*recA*$^+$); open triangles, MD425 (*recA*).

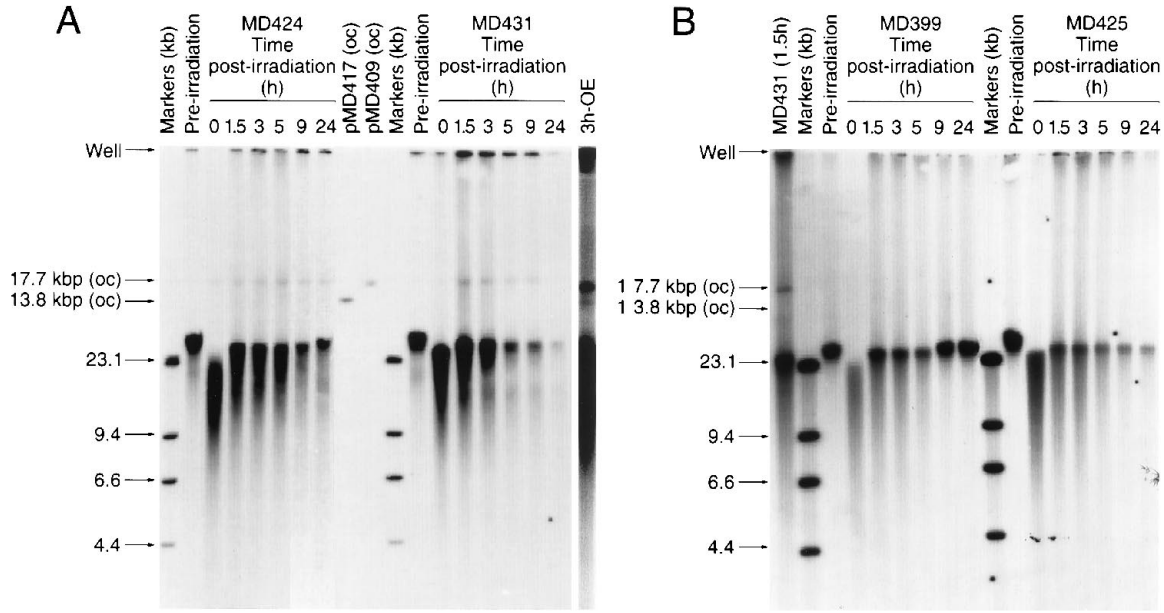

FIG. 5. (A) Generation of circular derivatives of repeated chromosomal fragments in *D. radiodurans* MD424 (*recA*$^+$) and MD431 (*recA*). Early-stationary-phase cultures were treated as described for Fig. 3. Each lane contains DNA from 3×10^6 cells, as determined by counting with a hemocytometer. Electrophoresis was in a 0.55% agarose gel for 12 h at 75 V before blotting and probing of the blot with a 1.2-kbp fragment of the pBR322 *tet* gene that had been radiolabeled with [^{32}P]dCTP by the random priming method. The markers include OC forms of pMD417 (13.8 kbp) (0.5 ng) and pMD409 (17.7 kbp) (0.5 ng), relaxed by in vitro γ radiation, and phage λ DNA digested with *Hin*dIII. 3h-OE, overexposed image of the 3-h lane of MD424 showing the 13.8- and 17.7-kbp OC forms. (B) Absence of circular derivatives of direct chromosomal insertions in *D. radiodurans* MD399 (*recA*$^+$) and MD425 (*recA*). Early-stationary-phase cultures were treated as described for Fig. 3 and then subjected to DNA electrophoresis and blotting as described for panel A. The sample labeled MD431 (1.5h) is the same DNA sample as that used in panel A.

diation samples, because the starting material is already shorter than what is generated by shear forces in the unirradiated samples.

All *recA* cells are reproductively dead following 1.75 Mrad (extrapolated survival of 10^{-15}) (Fig. 4), yet we have found that these cells increase their DNA size to about 3.0×10^4 bp, indicating that these cells have the capacity to mend about one-third of the DSBs during the first 1.5 h of postirradiation incubation in TGY medium (Fig. 3). However, at later times, no further repair occurred in the *recA* strain, but a gradual degradation of DNA size was found. This is illustrated in strain MD431 (*recA*) in Fig. 3. Strain MD424 (*recA*$^+$) shows the same initial enhancement of fragment size seen in MD431 (*recA*) occurring at 1.5 h postirradiation (Fig. 3). However, at later times, MD424 continued to show progressive enlargement of DNA fragments until they achieved the size of the control unirradiated DNA (Fig. 3). In MD424 (*recA*$^+$) cells, exponential growth begins about 12 h postirradiation (Fig. 4A). The growth lag following DNA damage is an intrinsic part of repair in *D. radiodurans*. It is accompanied by a limited amount of DNA degradation that depends on the extent of damage (for a review, see reference 21). The growth lag is dependent on the initial amount of damage and occurs in cells exposed to nonlethal (e.g., 0.5-Mrad) and partially lethal (e.g., 1.75-Mrad) DNA-damaging exposures and supports the presence of a prokaryotic checkpoint mechanism for DNA damage in *D. radiodurans* (2). Unlike strain MD424 cells the *recA* MD431 cells failed to show any further DSB mending after 1.5 h (Fig. 3), and there was no growth (Fig. 4A).

Irradiation induces circularization of chromosomal segments 417 and 409. Chromosomal reporter segments 417 and 409 could circularize after radiation exposure in *recA* cells by annealing regions of complementary single-stranded DNA. For example, the single-stranded DNA might be generated by digestion (resection) of 5′ strands within fragments of the repeated units. Such a ligation would result in a discrete open circular (OC) plasmid with a gel mobility representative of its size. These circles could be rescued in *E. coli* because of the *E. coli* pBR322 origin of replication and the *bla* gene (Ap^r) present in the plasmid sequences.

Included in Fig. 5A are two lanes containing pMD417 (13.8 kbp) and pMD409 (17.7 kbp), respectively, purified from *E. coli* and γ irradiated in vitro with 4 krad. This exposure was sufficient to relax the supercoiled plasmid standards to their respective OC forms. As such, they were used as size standards to indicate the positions of the predicted circular derivatives of segments 417 and 409. It can be seen from the postirradiation lanes in Fig. 5 that bands consistent with the presence of OC forms of segments 417 and 409 were generated in both strains MD424 (*recA*$^+$) and MD431 (*recA*) postirradiation.

In MD424, two of the predicted OC bands (13.8 kbp [pMD417] and 17.7 kbp [pMD409]) gain intensity following irradiation (Fig. 5A). These findings are reflected in the results obtained from transforming DNA from the individual DNA time point samples of Fig. 5A into *E. coli*; the number of Ap^r *E. coli* colonies obtained (Fig. 4B) generally corresponds to the intensity of the bands observed (Fig. 5A). The *recA* strain MD431 shows a similar production of circular forms after irradiation (Fig. 5A), indicating that circle formation is not *recA* dependent. This is most striking at the 1.5-h time point, where the amount of OC form and the number of Ap^r colonies derived from the same sample are greatest (compare Fig. 4 and 5A). Note that the lower OC form (13.8 kbp) in MD431 and MD424 is difficult to see in Fig. 5A; an overexposed autoradiogram of the same blot, however, demonstrates this band.

Structural analysis of the circular derivatives of segments 417 and 409. *E. coli*-derived sequences in segments 417 and 409 that contain an *E. coli* origin of replication are flanked by

identical repeats of deinococcal DNA when they are integrated into the *D. radiodurans* chromosome. As such, circular derivatives of segments 417 and 409, present in DNA samples prepared from cells, can be used to transform *E. coli* to Ap^r, as noted above. To assess the relative abundance of such circles in a given DNA sample, 1 μg of each of the genomic DNA samples from *recA*$^+$ and *recA D. radiodurans* cells used in Fig. 5A was transformed into *E. coli* DH10B. Selection was for the presence of the *bla* gene (Ap^r), which is present in both segments (Fig. 4B). Sixty of these Ap^r colonies were investigated by subjecting plasmids derived from those clones to detailed restriction mapping. All of the plasmids analyzed were rescued either before radiation or at 1.5 h postirradiation, well before a demonstrable RecA-mediated effect on strand rejoining was observed (Fig. 3 and 6). Plasmid structural analysis using *Pvu*II restriction digestion showed that all the plasmids investigated could have been generated either by annealing of complementary fragment ends in a non-*recA*-dependent reaction or by *recA*-dependent homologous recombination (Fig. 7). Eighty-five percent of the rescued circular forms had structures conforming exactly to either pMD409 (Fig. 7, column A) or pMD417 (column B). These two structures can be generated by annealing fragments liberated by DSBs occurring in regions of identity. The identical regions in the tandem duplications include both the chromosomal region (BC), much of the *E. coli* vector portions, and two different sequences derived from the *D. radiodurans* SARK natural plasmids pUE10 and pUE11 (Materials and Methods) (Fig. 7). The other plasmid structures detected (Fig. 7, columns C to E), which differ from both pMD417 and pMD409, are consistent with reannealing (occurring in pBR322-derived sequences) or *recA*-dependent recombination. Such fragments could give rise to plasmids in which the *cat* or *aphA* gene become linked to physical polymorphisms usually associated with the other drug resistance determinant. For example, column D in Fig. 7 shows data for clones in which *aphA* is linked to the 2.2-kbp rat cDNA polymorphism (this polymorphism is usually associated with *cat*). Two examples of a heterodimer were also obtained, with a structure consistent with the annealing of the ends of fragment F in Fig. 7. The data from analysis of circular products recovered by transformation into *E. coli* (Fig. 7) suggest that the 17.7- and 13.8-kbp circles are approximately equally common in MD424, yet the 17.7-kbp circles are visually more abundant than the 13.8-kbp circles in Fig. 5A. This may have resulted from a transformation phenomenon in which smaller plasmids are more readily taken up by cells than larger plasmids. If this is indeed the case, then the 13.8-kbp plasmids, while in low abundance in Fig. 5A, are highly represented among the transformants analyzed in Fig. 7.

Irradiation fails to induce circularization of the direct chromosomal insertion segment 399. The chromosomal direct insertion reporter segment 399 (Fig. 2) could circularize after an irradiation exposure in *recA*$^+$ and *recA* cells by random end-to-end joining of broken ends but not by a single-strand annealing (SSA)-type reaction that requires repeated sequences. Circularized chromosomal fragments containing the direct insertion Cm^r-Tc^s cassette could be rescued in *E. coli* because of the *E. coli* origin of replication and *bla* gene (Ap^r) present in the plasmid sequence. However, transformation into high-efficiency *E. coli* DH10B of DNA samples prepared from strains MD399 (*recA*$^+$) and MD425 (*recA*) before irradiation and during repair failed to give any transformants (Fig. 4). Neither increasing the transforming DNA concentration nor increasing the transformation efficiency of the DH10B competent cells resulted in the recovery of any transformants. Further, uncut DNA samples prepared from MD399 and MD425, recovering from 1.75-Mrad irradiation, failed to show evidence for OC derivatives of the direct insertion in Southern blots using the *tet* probe (Fig. 5B). Together, these results indicate that random end-to-end joining of broken DNA fragments is extremely rare, if not absent, in both *recA*$^+$ and *recA D. radiodurans.*

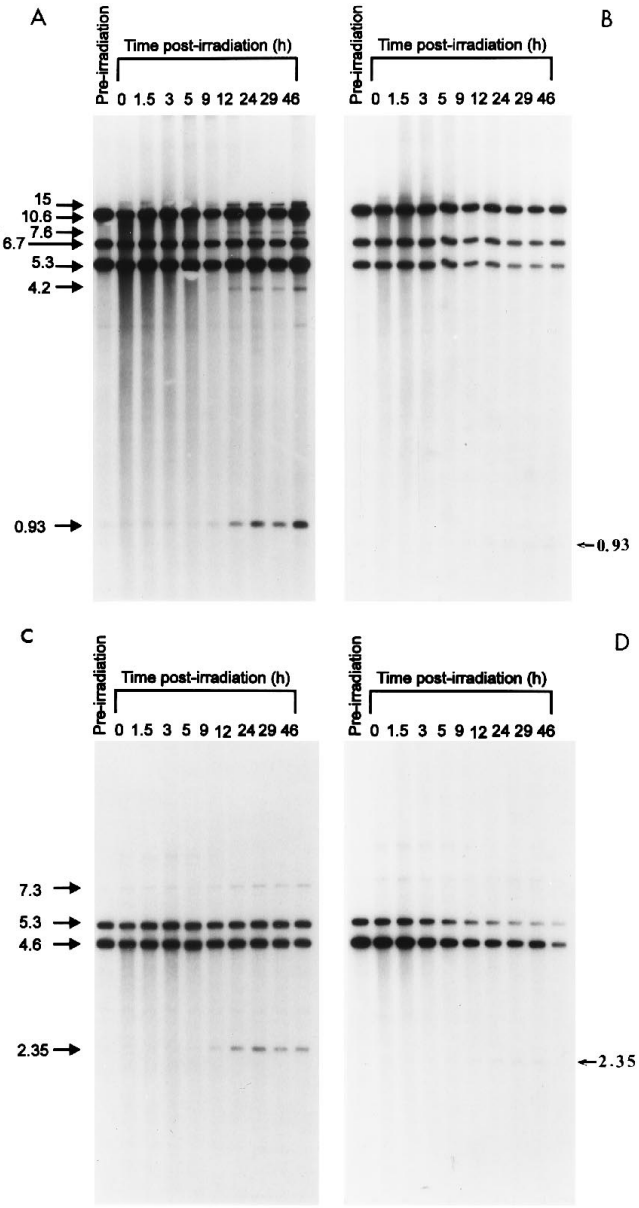

FIG. 6. Production of recombinant bands following irradiation of *D. radiodurans*. (A and C) MD424 (*recA*$^+$); (B and D) MD431 (*recA*). Cells were grown to the early stationary phase, irradiated, diluted 1/50 with fresh TGY, and allowed to recover without drug selection as described in the legend to Fig. 3. DNA was prepared from samples taken at the indicated times by the miniprep technique and cleaved with *Xho*I (A and B) or *Pvu*II (C and D). Each lane contains DNA from about 3×10^6 cells, as determined by hemocytometer count. Electrophoresis was in a 0.9% agarose gel for 18 h at 55 V (A and B) or in a 0.7% agarose gel at 55 V for 18 h (C and D) before blotting and probing. The blots were probed with the 1.2-kbp fragment of the *tet* gene that had been radiolabeled with [^{32}P]dCTP by the random priming method. The sizes of the parental and recombinant bands are indicated with arrows.

***recA*-dependent homologous recombination follows onset of *recA*-independent annealing.** The circularization of DNA fragments liberated by irradiation and recovered in *E. coli* as plasmid (Fig. 4, 5A, and 7) strongly suggests that the early *recA*-

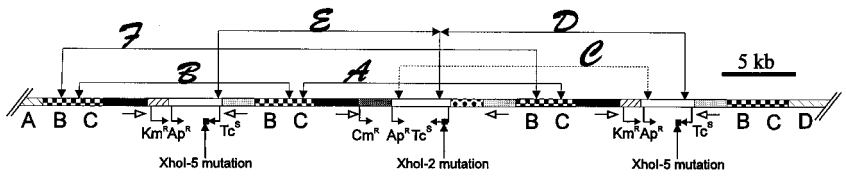

Source of DNA	No. of *E. coli* Ap^r colonies screened	Plasmid structure and size (kbp) 17.7 A	13.8 B	16.7 C	16.0 D	15.5 E	31.5 F
MD424 Preirradiation	14	8	5	1	0	0	0
MD424 Postirradiation 1.5 hr	12	4	7	0	0	1	0
MD431 Preirradiation	10	7	0	2	0	0	1
MD431 Postirradiation 1.5 hr	24	19	1	0	2	1	1

FIG. 7. Origin of Ap^r *E. coli* clones rescued from *D. radiodurans*. At the top is a structural representation of part of the MD424 and MD431 chromosomes, illustrating one of the many possible arrangements of the adjacently duplicated segments 417 (Km^r) and 409 (Cm^r) at locus 11. Segment shading is as described in the legend to Fig. 1. Regions A to F, marked above the chromosomal map, show examples of fragments which could be liberated by DSBs. If the ends of these indicated fragments become annealed, DNA circles which are able to replicate in *E. coli* as a result of the internal pBR322 replication origin are generated. Circular derivatives of fragments A to F represent all plasmid structures obtained after screening for Ap^r colonies. The table shows the number of plasmids identified as having structures which correspond to circularized forms of fragments A to F depicted at the top. The sizes of structures A to F are shown. The sources of DNA from which the Ap^r clones were originally derived are given on the left.

independent recombination pathway involves annealing of complementary single strands near the ends of the liberated fragments. This is further addressed in Discussion. The genetic system described here, using segments 417 and 409, has the advantage of being able to show the timing of the observed annealing events relative to the onset of *recA*-dependent recombination within the same cells.

Southern blot analysis of MD424 and MD431 chromosomal DNA permits the observation of recombination within specific windows in chromosomal DNA by virtue of restriction fragment length polymorphisms. In the case of *Xho*I restriction cleavage and probing with the *tet* gene, recombination within each of the four windows, X_1, X_2, X_3, and X_4 (Fig. 1C), yields new restriction fragments that can be detected on Southern blots (Fig. 1C and 6). At various times following a 1.75-Mrad exposure, total DNA was purified from non-drug-selective liquid cultures of MD424 (*recA*$^+$) and MD431 (*recA*) cells, cleaved with *Xho*I, and analyzed by Southern blot hybridization with the *tet* gene. The DNA samples analyzed in Fig. 5A and 6 are the same. The predicted recombinant fragments, each indicative of an event in one of four regions (Fig. 1C), are present in the autoradiogram of genomic DNA from the *recA*$^+$ strain MD424 (Fig. 6A). In particular, a 4.2-kbp fragment that occurs as the result of recombination within a 101-bp region between the *Xho*I-5 mutation and *Sty*I site is detectable as early as 9 h. This very small region of only 101 bp is indicated as X_2 in Fig. 1C. The most evident of the predicted recombinant bands in Fig. 6A is the 0.9-kbp fragment indicative of recombination in region X_3 in Fig. 1C. Its intensity increases dramatically after 9 h. The faint presence of the 0.9-kbp band in the preirradiation sample suggests that the sporadic rate of recombination in this region is high, possibly as a result of the proximity of segments 417 and 409 in a recombination-proficient host. In contrast, in the *recA* strain MD431, there is little evidence of recombinant bands (Fig. 6B); the 0.9-kbp band is slightly visible in the lanes corresponding to 9 to 46 h. We suggest that this band may be derived from a circular product of segments 417 and 409, generated by annealing fragments liberated by DSBs early in the course of recovery (similar to structure D in Fig. 7 in which the two different *Xho*I polymorphisms are linked); similar results would be obtained if two separate fragments with ends containing two different *tet* sequences (*Xho*I-2 and *Xho*I-5) annealed between the two mutations. Irrespective of whether a circle is formed, the fact that this band is slightly visible as late as 46 h suggests that the process of annealing fragments may be a continual one in *recA* cells, proceeding until such time as all DNA is degraded.

Recombination was also detectable between segments 417 and 409 by a *Pvu*II digestion of chromosomal DNA (MD424) using the same *tet* fragment as a probe. This procedure permits detection of restriction fragment length polymorphisms if a crossover occurs within the 1.37-kbp region marked X in Fig. 1B. The parental bands, representing segments that have not undergone recombination within this window, are 5.2 and 4.6 kbp and are nearly equally abundant, as demonstrated by the autoradiograms (Fig. 6C and D). Both of the predicted recombinant bands of 7.3 and 2.35 kbp (Fig. 1B) are also evident. The 2.35-kbp band is faintly visible as early as 5 h following irradiation and darker at later times in *recA*$^+$ MD424 (Fig. 6C). At early times postirradiation, the 7.3-kbp band is superimposed on a 7.5-kb partial digestion, but its presence is clearly evident by 9 h postirradiation. Because of the nature of the flanking polymorphisms and the *tet* probe used to observe the polymorphisms, the recombinant bands visible with a *Pvu*II digestion are the result of crossovers and not gene conversion. In *recA* strain MD431, there is little evidence of recombination; both the 7.3- and 2.35-kbp bands are slightly visible in the lanes corresponding to 5 to 46 h (Fig. 6D). As discussed above for the *Xho*I analysis of MD431, we suggest that these bands are derived from annealing products of segments 417 and 409.

The *recA*-dependent homologous recombination events described occur 5 or more h following irradiation and are com-

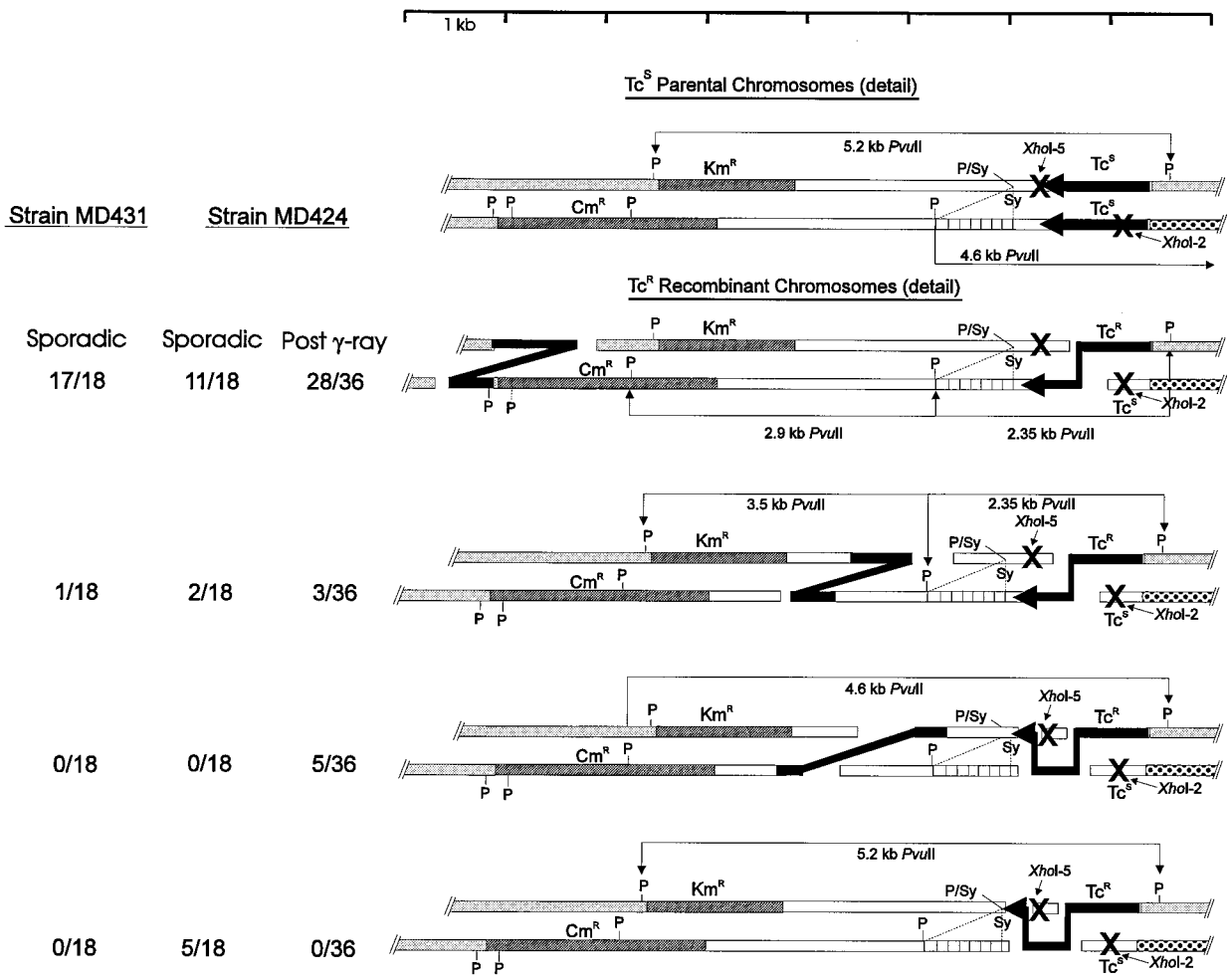

FIG. 8. Restriction enzyme analysis of Tc^r genomic segments arising sporadically and postirradiation in MD424 and MD431. There are no examples of postirradiation MD431 Tc^r colonies described because of radiolethality (see Fig. 4). At the top is a diagram of the two parental chromosomal segments 417 and 409, including those regions tested for recombination. DNA from cells from individual Tc^r recombinant colonies was prepared by the miniprep technique. DNA was cleaved with *Pvu*II and subjected to Southern blot analysis using the *tet* gene as a probe. The deduced structures of the recombinant segments, showing restriction cleavage sites and the simplest mechanism by which recombinational events could occur and be consistent with the diagnostic restriction fragments, are presented at the right. Segment shading and restriction site abbreviations are as described in the legend to Fig. 1. In addition, the heavy black lines indicate the *tet* gene, with the arrowhead giving the direction of transcription. Heavy black lines also indicate areas of reciprocal recombination. In the case of the parental segments, which contain the *Xho*I-2 or *Xho*I-5 mutation in the *tet* gene, this gene is labeled Tc^s, while in the recombinant structures, the *tet* genes are labeled Tc^r.

pletely consistent with the *recA* dependence observed in previous studies on interchromosomal recombination in *D. radiodurans* (5). These findings support the observations that reaction products consistent with annealing are seen in *D. radiodurans* predominantly at early times, i.e., 1.5 h (Fig. 3), and that at later times *recA*-dependent recombination predominates in *recA*$^+$ cells. Thus, the presumed annealing starts before *recA*-dependent recombination.

Structures of Tc^r conferring DNA segments in *D. radiodurans*. In addition to (i) measuring Ap^r transformation of *E. coli* DH10B and (ii) assessing physical polymorphisms in chromosomal DNA, another means of characterizing recombinational events is by selection for *D. radiodurans* Tc^r isolates pre- and postirradiation. While no postirradiation Tc^r recombinants were obtained in the *recA* strain MD431 (because of the lethal radiation exposure) (Fig. 4), Tc^r recombinants were obtained in *recA*$^+$ strain MD424 (spontaneous and postirradiation) and in MD431 (spontaneous) (Fig. 8). Tc^r recombinant cell counts of strain MD424 show that there is about a 10-fold increase in the frequency of Tc^r colonies relative to the sporadic preirradiation Tc^r frequency (Fig. 4). Total DNA prepared from pre- and 24-h postirradiation-induced Tc^r MD424 colonies and spontaneous MD431 Tc^r colonies was subjected to structural analysis by restriction endonuclease cleavage and Southern blotting using the *tet* gene as a probe. The structures of 36 Tc^r-conferring segments derived from irradiated *D. radiodurans* were compared with those of 18 sporadically occurring Tc^r-conferring segments of MD424 and 18 of MD431 (Fig. 8). In all cases, the most frequent event within this window of analysis was a single crossover in the 929-bp region between the *Xho*I-2 and *Xho*I-5 mutations in *tet* (28 of 36 [78%] of irradiated and 11 of 18 [61%] of control MD424 Tc^r recombinants and 17 of 18 [94%] of MD431 Tc^r control recombinants) (Fig. 8). The majority (62 of 72) of this group of Tc^r-conferring segments could not have arisen by gene conversion within *tet* because the recombinants lacked both of the flanking physical polymorphisms (the 695-kbp *Pvu*II-*Sty*I deletion of segment 417 and the 2.2-kbp rat DNA insertion of segment 409). In both the postirradiation and two preirradiation groups of Tc^r colonies, we found an unexpectedly high number of segments

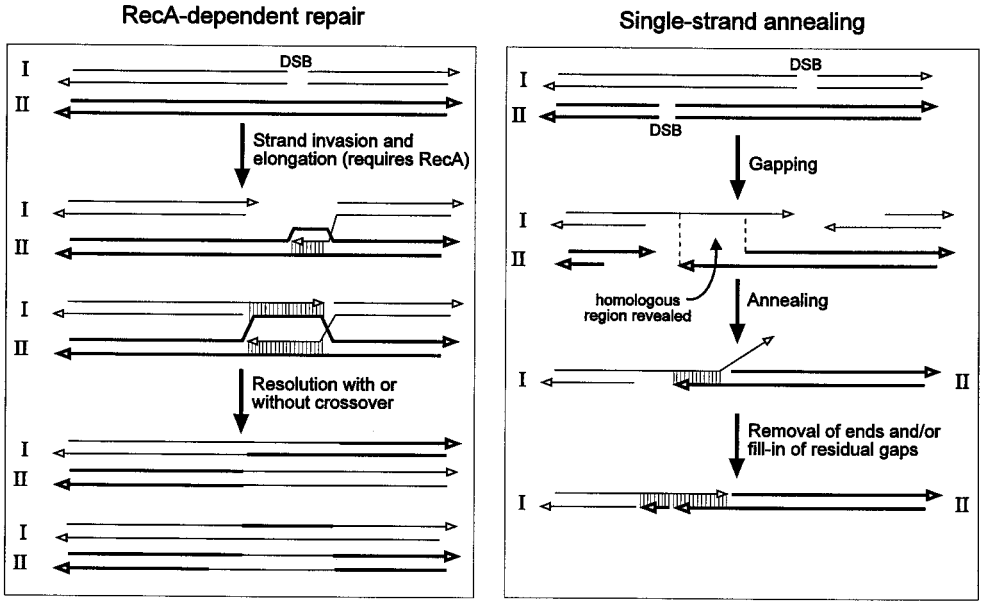

FIG. 9. Two pathways for DSB repair following γ irradiation. (A) Repair of a DSB by gene conversion or crossover between a DSB and a homologous uninterrupted DNA duplex. The pathway shown is based on a mechanism originally proposed for meiotic recombination in yeast cells (32). Exonucleolytic degradation of the 5′-to-3′ strand of the broken helix allows for RecA-mediated 3′-end strand invasion of the intact helix. After extension of this strand, the displaced strand serves as a template for resynthesis of the other broken strand. This configuration can be resolved with or without a crossover, in either case repairing the DSB. (B) Repair of a DSB by SSA. Following irradiation, there is exonucleolytic degradation of the 5′-to-3′ strands allowing for annealing of the remaining single strands. Nonhomologous ends are removed and any gaps are filled in, using the opposite strand as a template, to complete the SSA reaction (10, 14).

consistent with the occurrence of recombination in the 101-bp region between the *Xho*I-5 mutation and the *Pvu*II-*Sty*I deletion (Fig. 8). It was not possible to determine if the Tc^r segments in this group occurred by gene conversion or two closely linked crossovers within this window of observation.

DISCUSSION

The mechanism of recombinational DNA repair in *D. radiodurans* as determined by DNA fragment enlargement on PFGE in the first few hours following γ irradiation differs from that occurring over the next 24 h. The initial repair is not *recA* dependent, since it occurs to the same extent in both MD424 *recA*$^+$ and MD431 *recA* cells (Fig. 3). At later times, however, there is no enhancement of DNA fragment size in the *recA* cells, while in *recA*$^+$ cells, DNA fragments continue to enlarge until they are indistinguishable from preirradiation samples (Fig. 3). These results are the same as those reported previously for the repair of chromosomal DNA in wild-type *D. radiodurans* and its *recA* derivative rec30 (7). Therefore, it appears that increased DNA fragment size cannot be ascribed exclusively to *recA*-dependent repair but instead includes a different mode of repair at early times following γ irradiation. This other repair pathway is extremely efficient, since in the first 1.5 h it increases the average fragment size from about 20 to 30 kbp (Fig. 3), corresponding to a repair of about one-third of all DSBs.

Although many hypotheses may be advanced, we suggest that the initial increase in fragment size in *recA* and *recA*$^+$ derivatives may be due to a *recA*-independent SSA reaction similar to that thought to exist in *E. coli* (possibly in the RecE pathway) and *Saccharomyces cerevisiae* and other eukaryotes (10, 14, 26, 27) (Fig. 9). This pathway requires two partially identical chromosomal fragments in which the identical regions are rendered single stranded by exonucleases. By this means, complementary single-stranded regions from two different fragments (or the same fragment if rendered circular) are able to hybridize with each other in a *recA*-independent reaction. After hybridization, any nonhomologous ends could be removed by a DNA deoxyribophosphodiesterase (to eliminate radiolytic products at the broken DNA ends [23]), and any single-stranded gaps are presumably filled in by a DNA polymerase, followed by DNA ligation (10, 14, 26, 27). By annealing regions of identity or high homology, overall fragment sizes increase. Early annealing reactions would increase the physical length of many chromosomal DNA fragments, thereby reducing damage caused by exonucleases. Another benefit of increasing the length of substrate DNA might be that larger fragments are more easily engaged in RecA-mediated DNA repair.

***D. radiodurans* is proficient at *recA*-independent homologous joining of DNA ends.** The production of extrachromosomal circles that consist of segment 417 or 409 or both (Fig. 4, 5A, and 7) that can be rescued in *E. coli* (as a result of an *E. coli* origin of replication and Ap^r) occurs in both *D. radiodurans* *recA*$^+$ and *recA* cells (Fig. 4, 5A, and 7). Consequently, the formation of these circles is *recA* independent. Indeed, at early time points, the *recA* strain produces higher numbers of circles than the *recA*$^+$ strain (Fig. 4). In both strains, these circular forms persist for at least 9 h postirradiation and then disappear (Fig. 5A). The reduction in number of these circular forms in *recA*$^+$ cells during the exponential growth phase can be attributed to dilution of the DNA circles upon semiconservative replication, since these circles do not contain a deinococcal origin of replication.

Structural analysis of these *E. coli* plasmids (Fig. 7) showed that in all cases, they could have been derived by homologous annealing of fragments generated by DSBs within the chromosomal region containing the duplicated plasmids; there was no evidence for plasmids containing deletions or additions that

could be attributed to random end-to-end joining of broken chromosome ends (Fig. 7).

A genetic system that describes the timing of chromosomal *recA*-dependent repair has been reported recently for *D. radiodurans* (5). Under culture and radiation conditions identical to those used here and previously (5), we find that the onset of *recA*-dependent homologous recombination, as deduced by the appearance of recombinant bands, occurs around 5 h postirradiation (Fig. 6C). In *recA*$^+$ cells, the kinetics of DNA repair (Fig. 3), progress of recombination (Fig. 6), and assessment of individual crossover or gene conversion events (Fig. 8) are essentially identical to those *recA*$^+$ characteristics described in the earlier chromosomal study (5). In this study, therefore, the *recA*-dependent repair kinetics are unaffected by the presence of artificial tandem duplications at this chromosomal study locus. The results on timing of homologous recombination (Fig. 6), taken together with the data presented here on circular derivatives of the integrated plasmids, separate kinetically a *recA*-dependent effect, manifested between 5 and 9 h (Fig. 6), and the onset of a *recA*-independent SSA reaction starting within the first 1.5 h postirradiation (Fig. 5A).

Nonhomologous joining of DNA ends is extremely rare in *D. radiodurans*. The profound resistance of *D. radiodurans* to the mutagenic and lethal effects of ionizing radiation, together with the absence of examples of genomic deletions, insertions, or other rearrangements, is a characteristic of this organism consistent with a very low frequency of nonhomologous DNA end-joining (31).

We report here a direct test for the ability of radiation-induced nonrepetitive chromosomal fragments to recircularize by random end-to-end joining in *D. radiodurans recA*$^+$ and *recA* cells. We have reported previously (5) the construction of *D. radiodurans* strains containing direct chromosomal insertions of the Cm^r-Tc^s and Km^r-Tc^s gene cassettes used in this study (Fig. 1). MD399 (*recA*$^+$ [5]) and its *recA* equivalent MD425 (this study) both contain a direct chromosomal insertion of the Cm^r-Tc^s gene cassette (Fig. 2) at the same chromosomal location used to study repair of the repeated sequences in MD424 and MD431.

Following an exposure of MD399 (*recA*$^+$) and MD425 (*recA*) to 1.75 Mrad, we tested for the presence of circularized chromosomal fragments, containing the direct insertion Cm^r-Tc^s cassette, in DNA samples prepared from cells undergoing recovery (Fig. 4 and 5B). Transformation of DNA samples prepared from strains MD399 (*recA*$^+$) and MD425 (*recA*) before irradiation and during repair failed to give any *E. coli* DH10B transformants (Fig. 4). Further, uncut DNA samples prepared from MD399 and MD425, recovering from 1.75-Mrad irradiation, failed to show evidence for OC derivatives of the direct insertion in Southern blots using the *tet* probe (Fig. 5B). These circles, which would have arisen by blunt-end ligation, could have formed a smear in these blots in the region 20 to 30 kbp. However, such a smear was absent. This is in stark contrast to the results obtained for the tandemly duplicated sequences present in MD424 and MD431 (Fig. 4, 5A, and 7). Together, these results support the conclusions that (i) random end-to-end joining of broken chromosomal fragments is extremely rare, if not absent, in both *recA*$^+$ and *recA D. radiodurans* and (ii) recircularization of duplicated sequences occurs by a *recA*-independent sequence-specific DNA reaction (or SSA reaction).

These conclusions have been strengthened recently by DNA repair studies on *D. radiodurans* plasmids lacking any repeated sequences; such plasmids sustain as much damage per unit length as the chromosome following an in vivo exposure to 1.75 Mrad (7, 8). Under these conditions, the plasmids are linearized, but there is no evidence for any form of ligation of linearized plasmids in the first hours of recovery in either *recA*$^+$ or *recA* cells. Southern blot analysis of plasmid repair kinetics showed no evidence of plasmid recircularization (by DNA end joining) in the early hours of repair; also, these data show that the corresponding DNA samples from *D. radiodurans* were unable to transform *E. coli* to Ap^r. DNA from *recA* cells containing plasmid failed to transform *E. coli* at any time after irradiation. Furthermore, *recA*$^+$ *D. radiodurans* only showed the first evidence of repaired plasmid (by plasmid transformation) after 5 h, concomitant with the first evidence for *recA*-dependent recombination as demonstrated by plasmid DNA polymorphism studies (8).

SSA in the context of *recA*-dependent recombination. During the prolonged growth lag following high-dose irradiation, there is no obvious reason to stipulate that only one form of DSB repair is occurring. Our proposal that the earliest phase of DNA repair is dominated by SSA reactions, which continue through the lag phase, is supported by several observations: (i) fragmentation of the multiple chromosomes at high ionizing-radiation exposures yields small substrate DNA fragments of segments 417 and 409 suitable for SSA-mediated circularization, which is clearly observed in this study (Fig. 4, 5A, and 7); (ii) at the 1.5-h postirradiation time point, the sizes of the partially mended fragments in *recA*$^+$ and *recA* cells are identical (Fig. 3), providing no evidence for the onset of *recA*$^+$ recombination at this time (Fig. 6); (iii) the ongoing nature of the SSA reaction is supported by the faint presence of recombinant bands in the *recA* cells as seen at late times (Fig. 6); (iv) RecA is not detectable in undamaged *D. radiodurans* cells and is detectable only once cells are damaged, requiring a lag time for gene expression (4); and (v) the slowness of the appearance of the abundant recombinant bands as a result of *recA*$^+$-dependent recombination, as determined in strain MD424 (Fig. 1B, 1C, and 6), suggests that these events occur by a mechanism separate from and slower than that for SSA, consistent with the timing observed in prior interchromosomal recombination studies (5).

We have previously suggested that even an extraordinarily efficient recombination system cannot fully explain the radioresistance of *D. radiodurans* (20). To overcome the conceptual problem of how an apparently inevitable futile reinspection of fragments is avoided during *recA*-dependent recombinational repair, we have proposed that the *D. radiodurans* multiple chromosomes are aligned (6, 20). An SSA pathway would clearly also work very efficiently in the context of such a chromosomal alignment.

ACKNOWLEDGMENT

This work was supported by USPHS grant GM39933.

REFERENCES

1. **Anderson, A. W., H. C. Nordon, R. F. Cain, G. Parrish, and D. Duggan.** 1956. Studies on a radio-resistant micrococcus. I. Isolation, morphology, cultural characteristics, and resistance to gamma radiation. Food Technol. **10:**575–578.
2. **Bridges, B. A.** 1995. Are there DNA damage checkpoints in *E. coli*? Bioessays **17:**63–70.
3. **Brosius, J.** 1984. Plasmid vectors for the selection of promoters. Gene **27:**151–160.
4. **Carroll, J. D., M. J. Daly, and K. W. Minton.** 1996. Expression of *recA* in *Deinococcus radiodurans*. J. Bacteriol. **178:**130–135.
5. **Daly, M. J., and K. W. Minton.** 1995. Interchromosomal recombination in the extremely radioresistant bacterium *Deinococcus radiodurans*. J. Bacteriol. **177:**5495–5505.
6. **Daly, M. J., and K. W. Minton.** 1995. Resistance to radiation. Science **270:**1318.
7. **Daly, M. J., L. Ouyang, P. Fuchs, and K. W. Minton.** 1994. In vivo damage and *recA*-dependent repair of plasmid and chromosomal DNA in the radi-

ation-resistant bacterium *Deinococcus radiodurans*. J. Bacteriol. **176:**3508–3517.
8. **Daly, M. J., L. Ouyang, and K. W. Minton.** 1994. Interplasmidic recombination following irradiation of the radioresistant bacterium *Deinococcus radiodurans*. J. Bacteriol. **176:**7506–7515.
9. **Doherty, M. J., P. T. Morrison, and R. Kolodner.** 1983. Genetic recombination of bacterial plasmid DNA: physical and genetic analysis of the products of plasmid recombination in *Escherichia coli*. J. Mol. Biol. **167:**539–560.
10. **Fishman-Lobell, J., and J. E. Haber.** 1992. Removal of nonhomologous DNA ends in double-strand break recombination: the role of the yeast ultraviolet repair gene *RAD1*. Science **258:**480–484.
11. **Gutman, P. D., J. D. Carroll, C. I. Masters, and K. W. Minton.** 1994a. Sequencing, targeted mutagenesis and expression of a *recA* gene required for the extreme radioresistance of *Deinococcus radiodurans*. Gene **141:**31–37.
12. **Gutman, P. D., P. Fuchs, and K. W. Minton.** 1994b. Restoration of the DNA damage resistance of *Deinococcus radiodurans* DNA polymerase mutants by *Escherichia coli* DNA polymerase 1 and Klenow fragment. Mutat. Res. **314:**87–97.
13. **Gutman, P. D., H. Yao, and K. W. Minton.** 1991. Partial complementation of the UV sensitivity of *Deinococcus radiodurans* excision repair mutants by the cloned *denV* gene bacteriophage T4. Mutat. Res. **254:**207–215.
14. **Haber, J. E.** 1992. Exploring the pathways of homologous recombination. Curr. Opin. Cell Biol. **4:**401–412.
15. **Hansen, M. T.** 1978. Multiplicity of genome equivalents in the radiation-resistant bacterium *Micrococcus radiodurans*. J. Bacteriol. **134:**71–75.
16. **Lennon, E., and K. W. Minton.** 1990. Gene fusions with *lacZ* by duplication insertion in the radioresistant bacterium *Deinococcus radiodurans*. J. Bacteriol. **172:**2955–2961.
17. **Masters, C. I., and K. W. Minton.** 1992. Promoter probe and shuttle plasmids for *D. radiodurans*. Plasmid **28:**258–261.
18. **Masters, C. I., M. D. Smith, P. D. Gutman, and K. W. Minton.** 1991. Heterozygosity and instability of amplified chromosomal insertions in the radioresistant bacterium *Deinococcus radiodurans*. J. Bacteriol. **173:**6110–6117.
19. **Minton, K. W.** 1994. DNA repair in the extremely radioresistant bacterium *Deinococcus radiodurans*. Mol. Microbiol. **13:**9–15.
20. **Minton, K. W., and M. J. Daly.** 1995. A model for repair of radiation-induced DNA double-strand breaks in the extreme radiophile *Deinococcus radiodurans*. Bioessays **17:**457–464.
21. **Moseley, B. E. B.** 1983. Photobiology and radiobiology of *Micrococcus* (*Deinococcus*) *radiodurans*. Photochem. Photobiol. Rev. **7:**223–274.
22. **Moseley, B. E. B., and H. J. R. Copland.** 1975. Isolation and properties of a recombination-deficient mutant of *Micrococcus radiodurans*. J. Bacteriol. **121:**42–428.
23. **Mun, C., J. Rowe, M. Sandigursky, K. W. Minton, and W. A. Franklin.** 1994. DNA deoxyribophosphodiesterase and an activity that cleaves DNA containing thymine glycol adducts in *Deinococcus radiodurans*. Radiat. Res. **138:**282–285.
24. **Pyle, L. E., L. N. Corcoran, B. G. Cocks, A. D. Bergman, J. C. Whitley, and L. R. Finch.** 1988. Pulsed field electrophoresis indicates larger-than-expected sizes for the mycoplasma genomes. Nucleic Acids Res. **16:**6015–6025.
25. **Resnick, M. A.** 1978. Similar responses to ionizing radiation of fungal and vertebrate cells and the importance of DNA double-strand breaks. J. Theor. Biol. **71:**339–346.
26. **Silberstein, Z., M. Shalit, and A. Cohen.** 1993. Heteroduplex strand-specificity in restriction-stimulated recombination by the RecE pathway of *Escherichia coli*. Genetics **133:**439–448.
27. **Silberstein, Z., Y. Tzfati, and A. Cohen.** 1995. Primary products of break-induced recombination by *Escherichia coli* RecE pathway. J. Bacteriol **177:**1692–1698.
28. **Smith, M. D., R. Abrahamson, and K. W. Minton.** 1989. Shuttle plasmids constructed by the transformation of an *Escherichia coli* cloning vector into two *Deinococcus radiodurans* plasmids. Plasmid **22:**132–142.
29. **Smith, M. D., E. Lennon, L. B. McNeil, and K. W. Minton.** 1988. Duplication insertion of drug resistance determinants in the radioresistant bacterium *Deinococcus radiodurans*. J. Bacteriol. **170:**2126–2135.
30. **Smith, M. D., C. I. Masters, E. Lennon, L. B. McNeil, and K. W. Minton.** 1991. Gene expression in *Deinococcus radiodurans*. Gene **98:**45–52.
31. **Sweet, D. M., and B. E. B. Moseley.** 1976. The resistance of *Micrococcus radiodurans* to killing and mutation by agents which damage DNA. Mutat. Res. **34:**175–186.
32. **Szostak, J. W., T. L. Orr-Weaver, R. J. Rothstein, and F. W. Stahl.** 1983. The double-strand break model for recombination. Cell **33:**25–35.